



# CAS 2026

## Basic Science Abstracts

## Contents

<b>Non-invasive assessment of cardiac oxygenation using photoacoustic imaging .....</b>	<b>3</b>
<b>Toward EEG-based monitoring of anesthetic depth using information decomposition .....</b>	<b>6</b>

# Non-invasive assessment of cardiac oxygenation using photoacoustic imaging

## Submission ID

185

## AUTHORS

Noble, Ronan;<sup>1,2</sup> Vu, Jennie,<sup>2,3,4</sup> Khodabocus, Ibrahim;<sup>2,3,5</sup> Derzi, Simone;<sup>6</sup> Henry, Matthew;<sup>5,7</sup> Bourque, Stephane<sup>2,3,4,5,6,7</sup>

<sup>1</sup>Department of Anesthesiology, Perioperative and Pain Medicine, Cumming school of medicine, University of Calgary; <sup>2</sup>Women and Children's Health Research Institute, University of Alberta, Edmonton, Canada; <sup>3</sup>Cardiovascular Research Institute, University of Alberta, Edmonton, Canada; <sup>4</sup>Department of Physiology, University of Alberta, Edmonton, Canada; <sup>5</sup>Department of Pediatrics, University of Alberta, Edmonton, Alberta, Canada; <sup>6</sup>Department of Anesthesiology and Pain Medicine, University of Alberta, Edmonton, Alberta, Canada; <sup>7</sup>Division of Pediatric Cardiology, University of Alberta, Edmonton, Canada

## INTRODUCTION

Perioperative incidents such as hypoxic cardiac injury, present significant diagnostic challenges due to their often subtle or nonspecific clinical presentation [1]. However, reductions in myocardial oxygenation and perfusion precedes biochemical changes, as well as changes in ECG and wall motion abnormalities [2,3]. Photoacoustic imaging (PAI) is a modality that uses laser irradiation of a tissue to generate ultrasonic waves, which can then be detected by ultrasound. PAI enables spatially resolved quantitative mapping of various molecules, such as oxygenated and deoxygenated hemoglobin (based on their differential absorption spectra of 850 and 750 nm respectively) [4]. The objective of this study was to evaluate the application of PAI in monitoring oxygenation of the myocardium and great vessels and benchmark its performance against conventional ECG and echocardiography as a potential early warning sign for myocardial hypoxemia. We then sought to test the myocardial response to select vasoactive and inotropic agents.

## METHODS

Male CD-1 Elite mice were positioned supine and anesthetized with isoflurane (4% induction, 2% maintenance) carried in 1 L/min medical-grade gas (composition described below), as previously described [5]. Four imaging protocols were conducted in three separate cohorts of mice. Photoacoustic and simultaneous B-mode ultrasound images of the myocardium and right ventricular outflow tract (RVOT), as well as the pulmonary artery and aorta were acquired at steady states with a fractional inspired oxygen fraction (FiO<sub>2</sub>) of 21% (medical grade air) and then 100% (medical grade oxygen). In the same cohort of mice, the FiO<sub>2</sub> was then reduced to 10% for 60 seconds by introducing medical grade nitrogen

using a gas mixer, and then restored to 100%. A second cohort of mice were anesthetized and instrumented with a 26G IV. Photoacoustic and simultaneous B-mode ultrasound images of the myocardium and right ventricular outflow tract (RVOT) were again recorded. Mice received IV phenylephrine and isoproterenol at a 2:1 ratio doubling every 8 minutes. Finally, in a third cohort of mice the individual effects of various inotropes and vassopressors were assessed. Each mouse was given increasing doses of phenylephrine, isoproterenol, or norepinephrine. Each protocol was stopped when myocardial oxygen saturation decreased by ~50%.

## RESULTS

PAI reliably distinguished changes in oxygenation in the myocardium, RVOT chamber, aorta, and pulmonary artery when the  $FiO_2$  was changed from 100% to 21% ( $P < 0.0001$ ) and from 21% to 10% ( $P < 0.0001$ ). With escalating doses of phenylephrine and isoproterenol a progressive myocardial desaturation as well as decreasing RVOT oxygenation occurred (-50%,  $P < 0.001$ ). Importantly, we found when the myocardium is stressed its oxygen saturation drops below that of the RVOT oxygen saturation indicating the unique sensitivity of the heart ( $P < 0.01$ ). Cardiac contractility, measured from B-mode ultrasound, did not significantly reduce until myocardial oxygenation decreased by 17% ( $P < 0.05$ ). Further, PAI detected a 10% reduction in myocardial oxygenation prior to the onset of ECG abnormalities ( $P < 0.05$ ). Finally, we tested the response to individual agents. Isoproterenol ( $P < 0.01$ ) and phenylephrine ( $P < 0.001$ ) alone each caused a more rapid desaturation than when the agents were given together. Mice demonstrated a greater tolerance to norepinephrine than phenylephrine or a combination of isoproterenol and phenylephrine.

## DISCUSSION

While PAI is presently studied in humans for other purposes, the ability to measure oxygenation within the aorta and pulmonary artery has the potential to offer a more central measure of oxygenation than conventional pulse oximetry, as well as serve as a non-invasive measure of oxygen extraction. This work also demonstrates the potential for PAI to be integrated into the existing monitoring armamentarium, as it may offer an earlier warning of cardiac dysfunction and injury compared to existing monitoring devices. Finally, this work compared various pharmacological agents and showed how at large doses norepinephrine may be preferred over phenylephrine.

## REFERENCES

1. Wittmann M, Dinc T, Kunsorg A, Marcucci M, Ruetzler K. Preventing, identifying and managing myocardial injury after non cardiac surgery - a narrative review. *Curr Opin Anaesthesiol.* 2025 Feb 1;38(1):17-24. doi: 10.1097/ACO.0000000000001454.
2. Landesberg G, Mosseri M, Wolf Y, Vesselov Y, Weissman C. Perioperative myocardial ischemia and infarction: identification by continuous 12-lead electrocardiogram with

online ST-segment monitoring. *Anesthesiology*. 2002 Feb;96(2):264-70. doi: 10.1097/00000542-200202000-00007.

3. Arnold JR, Karamitsos TD, Bhamra-Ariza P, Francis JM, Searle N, Robson MD, Howells RK, Choudhury RP, Rimoldi OE, Camici PG, Banning AP, Neubauer S, Jerosch-Herold M, Selvanayagam JB. Myocardial oxygenation in coronary artery disease: insights from blood oxygen level-dependent magnetic resonance imaging at 3 tesla. *J Am Coll Cardiol*. 2012 May 29;59(22):1954-64. doi: 10.1016/j.jacc.2012.01.055.
4. Attia ABE, Balasundaram G, Moothanchery M, Dinish US, Bi R, Ntziachristos V, Olivo M. A review of clinical photoacoustic imaging: Current and future trends. *Photoacoustics*. 2019 Nov 7;16:100144. doi: 10.1016/j.pacs.2019.100144.
5. Noble RMN, Kirschenman R, Wiedemeyer A, Patel V, Rachid JJ, Zemp RJ, Davidge ST, Bourque SL. Use of Photoacoustic Imaging to Study the Effects of Anemia on Placental Oxygen Saturation in Normoxic and Hypoxic Conditions. *Reprod Sci*. 2024 Apr;31(4):966-974. doi: 10.1007/s43032-023-01395-6.

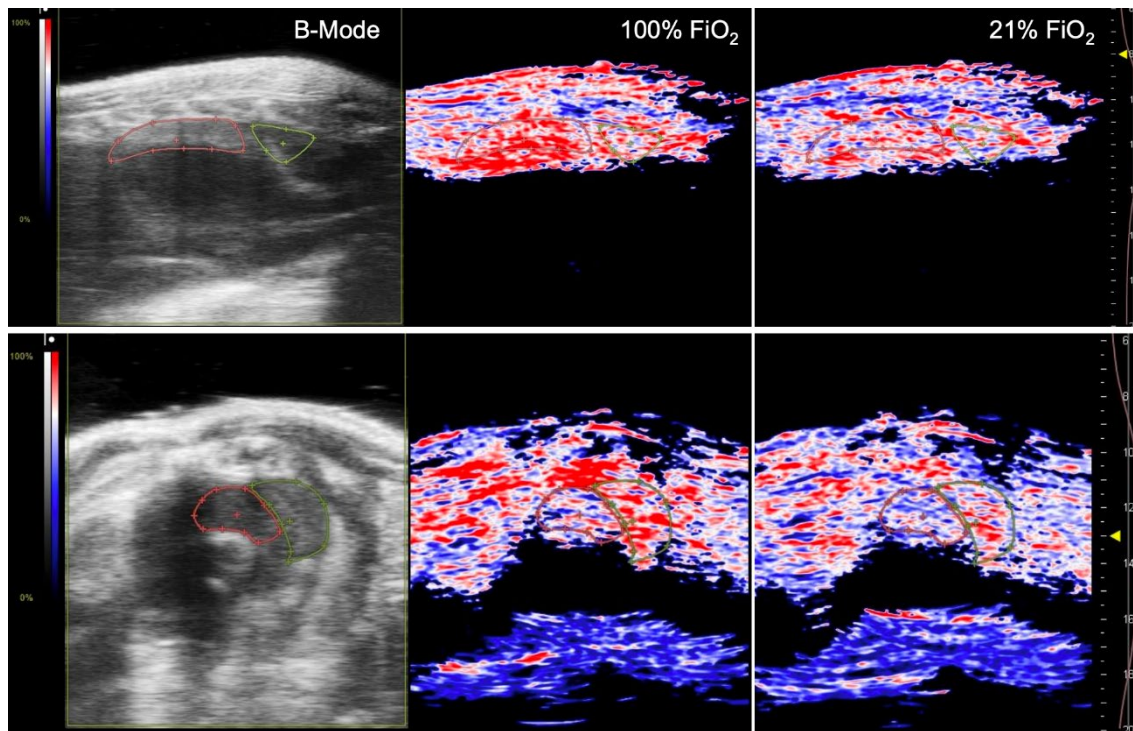


Figure 1

# Toward EEG-based monitoring of anesthetic depth using information decomposition

## Submission ID

39

## AUTHORS

Streicher, Joaquim;<sup>1,3</sup> Liardi, Alberto;<sup>2</sup> Bazregarzadeh, Hanieh;<sup>3</sup> Lahaie, Loudrick;<sup>1,3</sup> Newman, Derek;<sup>4</sup> Martin, Antonio;<sup>3</sup> Blackburne, George;<sup>5</sup> Godin, Nadia;<sup>6</sup> Verdonck, Olivier;<sup>1,6</sup> Carrier, Julie;<sup>1,3</sup> Lina, Jean-Marc;<sup>3,7</sup> Richebé, Philippe;<sup>1,8</sup> Morisson, Louis;<sup>1,6</sup> Mediano, Pedro A.;<sup>2</sup> Duclos, Catherine<sup>1,3</sup>

<sup>1</sup>Université de Montréal, Montréal, Canada; <sup>2</sup>Imperial College London, London, UK; <sup>3</sup>Center for Advanced Research in Sleep Medicine, Hôpital du Sacré-Cœur de Montréal, CIUSSS du Nord-de-l'île-de-Montréal, Montréal, Canada; <sup>4</sup>McGill University, Montréal, Canada; <sup>5</sup>University College London, London, UK; <sup>6</sup>Hôpital Maisonneuve-Rosemont, CIUSSS de l'Est-de-l'île-de-Montréal, Montréal, Canada; <sup>7</sup>École de technologie supérieure, Montréal, Canada; <sup>8</sup>Polyclinique Bordeaux Nord Aquitaine, Bordeaux, France

## INTRODUCTION

A growing body of evidence indicates that improper titration of general anesthesia—whether too light or too deep—can be harmful, leading either to rare cases of intraoperative awareness<sup>1</sup> or to increased morbidity and delayed neurocognitive recovery.<sup>2</sup> Although awareness occurs in only 0.1–0.2% of cases,<sup>1</sup> it carries a serious risk of long-term psychological distress, including post-traumatic stress disorder.<sup>3</sup> There is therefore a strong need for reliable, objective measures of anesthesia depth, such as those based on electroencephalography (EEG).

Recent work shows that information-theoretic measures—particularly synergy, reflecting interactions among brain regions, and redundancy, reflecting shared information—track changes in consciousness during anesthesia using fMRI.<sup>4</sup> We previously extended this framework to high-density (128-channel) EEG, demonstrating sensitivity to anesthesia-induced changes in information processing (unpublished). Here, we test whether these metrics remain effective when applied to sparse clinical EEG configurations ( $n = 24$  and  $n = 2$  electrodes).

## METHODS

We recorded high-density EEG from eight surgical patients in the operating room. All participants received propofol anesthesia, initiated at a target effect-site concentration of 2.0  $\mu\text{g/mL}$  and titrated in 0.2  $\mu\text{g/mL}$  steps to maintain a Bispectral Index (BIS) between 45 and 55. EEG data were down-sampled to 250 Hz, band-pass filtered (0.1–50 Hz), and

cleaned by removing noisy channels and contaminated time segments based on visual inspection.

Preprocessed EEG data were analyzed using the Integrated Information Decomposition ( $\phi$ ID) framework, which decomposes the mutual information between collections of electrodes and a target variable—defined here as the temporal evolution from past to future signal states—into unique, redundant, and synergistic components.<sup>5</sup> Signals from selected electrodes were averaged to form two virtual sensors representing the information sources. We examined two spatial partitions of the scalp (left–right and frontal–posterior), each implemented at two montage densities. In the 24-electrode configuration, 12 electrodes were assigned to each region, selected across all patients after excluding noisy channels, while preserving spatial coverage and symmetry as much as possible. In the 2-electrode configuration, a single electrode was assigned to each region, forming a BIS-like montage that allowed us to test the robustness of the metrics under clinically realistic EEG setups.

## RESULTS

In the 24-electrode configuration, interhemispheric decomposition revealed significant effects for redundant ( $t = 5.25$ ,  $p = 0.0012$ ) and synergistic components ( $t = 2.66$ ,  $p = 0.033$ ), but not for the unique component ( $t = 0.79$ ,  $p = 0.46$ ) (Figure 1A). In the front–back decomposition, anesthesia increased redundant information ( $t = 4.31$ ,  $p = 0.0035$ ), while neither unique ( $t = 0.40$ ,  $p = 0.70$ ) nor synergistic ( $t = 2.21$ ,  $p = 0.063$ ) components were significant (Figure 1B).

In the two-electrode configuration, unique information was significant for left–right decomposition ( $t = 4.68$ ,  $p = 0.0023$ ), whereas redundancy ( $t = 1.56$ ,  $p = 0.16$ ) and synergy ( $t = 0.55$ ,  $p = 0.60$ ) were not (Figure 1C). Using anterior and posterior electrodes as sources, all components were significant: unique ( $t = 2.55$ ,  $p = 0.038$ ), redundant ( $t = 3.26$ ,  $p = 0.014$ ), and synergistic ( $t = 2.65$ ,  $p = 0.033$ ) (Figure 1D).

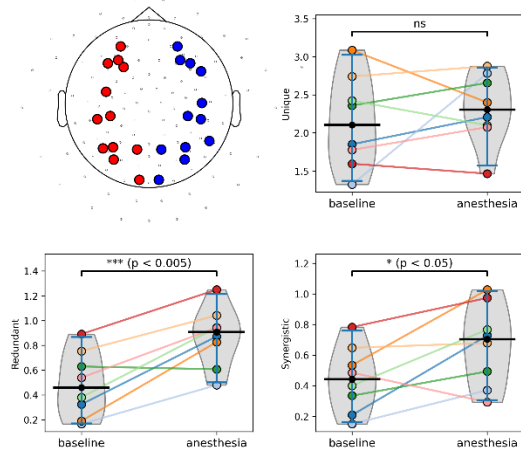
## DISCUSSION

In contrast to our previous results with the full electrode set—where interhemispheric redundancy and front–back unique information increased under general anesthesia—these findings highlight region-specific effects and the importance of electrode selection. Nevertheless, the recovery of meaningful patterns from sparse electrode configurations underscores the strong clinical potential of these measures. Future work should apply these methods directly to BIS data and refine synergy estimation by accounting for inter-electrode correlations that may inflate redundancy and underestimate synergy. Alternative computational approaches and source-space analyses will be essential to further clarify these effects and advance the development of reliable anesthesia depth monitoring tools.

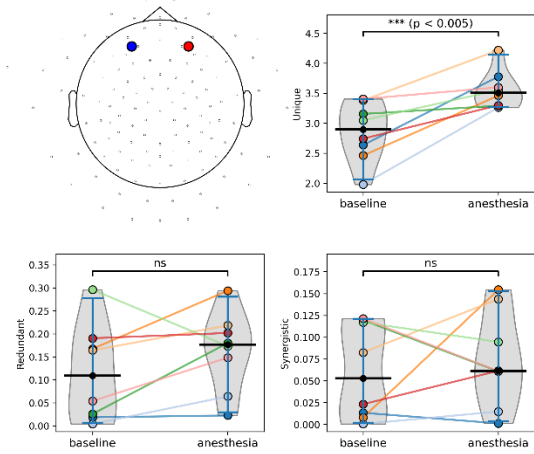
## REFERENCES

1. Sebel, P. S., Bowdle, T. A., Ghoneim, M. M., Rampil, I. J., Padilla, R. E., Gan, T. J., & Domino, K. B. (2004). The incidence of awareness during anesthesia: A multicenter United States study. *Anesthesia & Analgesia*, 99(3), 833–839. <https://doi.org/10.1213/01.ANE.0000130261.90896.6C>
2. Chan, M. T. V., Cheng, B. C. P., Lee, T. M. C., Gin, T., & CODA Trial Group. (2013). BIS-guided anesthesia decreases postoperative delirium and cognitive decline. *Journal of Neurosurgical Anesthesiology*, 25(1), 33–42. <https://doi.org/10.1097/ANA.0b013e3182712fba>
3. Osterman, J. E., Hopper, J., Heran, W. J., Keane, T. M., & van der Kolk, B. A. (2001). Awareness under anesthesia and the development of posttraumatic stress disorder. *General Hospital Psychiatry*, 23(4), 198–204. [https://doi.org/10.1016/S0163-8343\(01\)00142-6](https://doi.org/10.1016/S0163-8343(01)00142-6)
4. Luppi, A. I., Mediano, P. A. M., Rosas, F. E., Allanson, J., Pickard, J., Carhart-Harris, R. L., Williams, G. B., Craig, M. M., Finoia, P., Owen, A. M., Naci, L., Menon, D. K., Bor, D. & Stamatakis, E. A. (2024). A synergistic workspace for human consciousness revealed by integrated information decomposition. *eLife*, 12, RP88173. <https://doi.org/10.7554/eLife.88173.4>
5. Mediano, P. A. M., Rosas, F. E., Luppi, A. I., Carhart-Harris, R. L., Bor, D., Seth, A. K., & Barrett, A. B. (2025). Toward a unified taxonomy of information dynamics via integrated information decomposition. *Proceedings of the National Academy of Sciences*, 122(39), e2423297122. <https://doi.org/10.1073/pnas.2423297122>

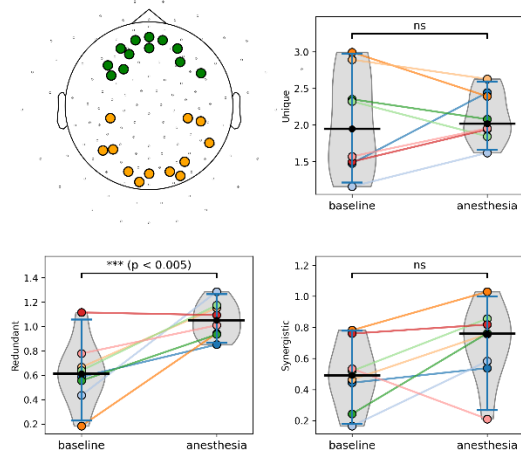
**A) Left-right spatial partition (n=24)**



**C) Left-right spatial partition (n=2)**



**B) Front-back spatial partition (n=24)**



**D) Front-back spatial partition (n=2)**

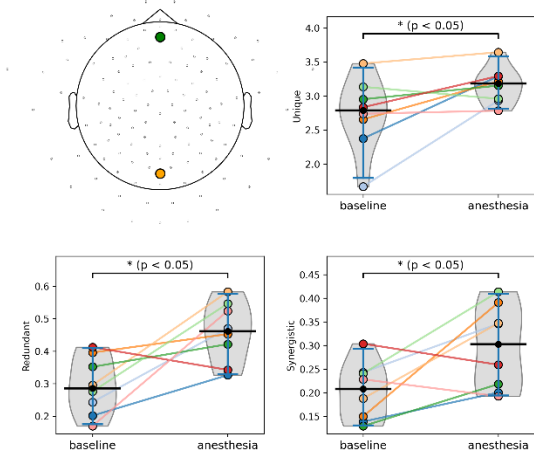


**Figure 1. Information decomposition across left-right and front-back axes using electrode subsets (n=24 and n=2)**

Unique, redundant, and synergistic information for baseline versus propofol anesthesia. Black horizontal bars show medians, blue vertical bars show 95% confidence intervals (CI), and colored dots/lines represent individual subjects across states.